공학석사학위논문

자가세정과 김서림 방지 기능을 갖는 투명한 omniphobic 유리 제작 및 평가

Fabrication and evaluation of omniphobic transparent glass with self-cleaning and anti-fogging capability

2015 년 8 월

서울대학교 대학원

기계항공공학부

손 태 호

Abstract

Fabrication and evaluation of omniphobic transparent glass with self-cleaning and anti-fogging capability

Taeho Son
Department of Mechanical and Aerospace Engineering
The Graduate School
Seoul National University

It is well known that superhydrophobic surfaces, having an apparent contact angle of water higher than 150° and low contact angle hysteresis, show a self-cleaning property, i.e. lotus effect. However these surfaces are vulnerable to oil contamination and in contaminated by oil. their self-cleaning property deteriorate. Therefore, it is vital for the surfaces to be omniphobic, Here we fabricate, optimize, and test omniphobic transparent glass prepared by non-lithographic, anisotropic etching. In order to make surface roughness and lower surface energy, a glow discharge of CF_4 gas and 1*H*,1*H*,2*H*,2*H*-perfluorooctyl trichlorosilane (PFOTS) were used, respectively. We investigate the effect of temperature, CF_4 plasma duration, and PFOTS vapor deposition time on the contact angles of water, ethylene glycol, and hexadecane. The results of measurements of the contact angle were also compared with theory of Cassie and Baxter. Finally, optical transmission for several glass was measured to quantify self-cleaning and anti-fogging.

keywords : superhydrophobic, omniphobic, glass, plasma, self-cleaning, anti-fogging
Student Number : 2013-23071

Contents

List of Figures

List of Tables

1 Introduction

Many superhydrophobic surfaces in nature such as lotus leaf [1], water strider's leg [2], mosquito eye [3] have been studied and it was found that theses surfaces are composed of surface roughness and chemical substance having low surface energy. Inspired by these studies, there are many attempts to fabricate biomimetic superhydrophobic surfaces by using laser [4], dip-coating [5], layer-by-layer [6], plasma [7, 8], etc.

However, superhydrophobic surfaces are prone to contamination of oil with a surface tension lower than that of water, and if contaminated by oil, they lose self-cleaning property. Hence, it is essential for the surfaces to be oleophobic. There are several omniphobic glasses by using layer-by-layer [6] and plasma [7], as shown in Figure 1.1 and Figure 1.2, respectively. In many cases, the preparation methods of omniphobic glass suggested thus far require many additional steps such as sol-gel and lithography processes. Furthermore, the additionally added nanostructure and the substrate are not of the identical materials [5-7], leading to intrinsic problem of durability.

Only a few glasses whose nanostructure is identical to the substrate have been reported. [4, 8] In microstructured glass, transparency problem occurs, as shown in Figure 1.3 [4]. Therefore, in order to obtain transparency, it is necessary for glass to have nanostructure. When nanostructure is formed on glass, transparency problem does not occur but too many additional steps are needed, as shown in Figure 1.4 [8].

In this study, we fabricate and optimized omniphobic transparent glass by modifying a non-lithographic, anisotropic

etching method. Furthermore, we quantify the effects of wettability of glass on the self-cleaning and anti-fogging with optical transmission.

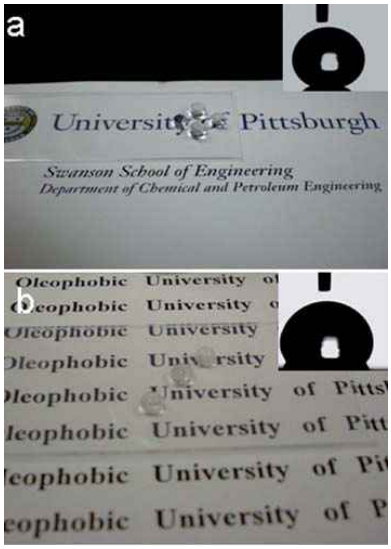

Figure 1.1 Photographs of a coated glass slide with droplets of (a) water and (b) hexadecane to demonstrate the superhydrophobicity, high oil-repellency, and transparency of the coating. (Cao *et al.*, 2010)

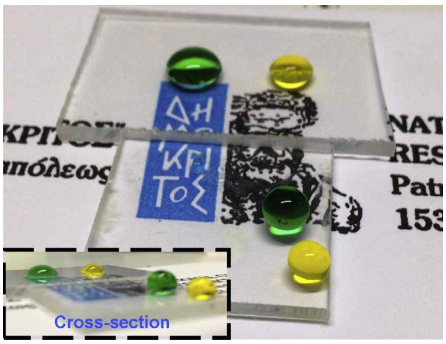

Figure 1.2 Photo of treated (bottom) and untreated (top) samples with liquid drops on them Notice the difference in the two samples for water (green) and lower surface tension liquid (yellow) drops. (Kontziampasis *et al.*, 2014)

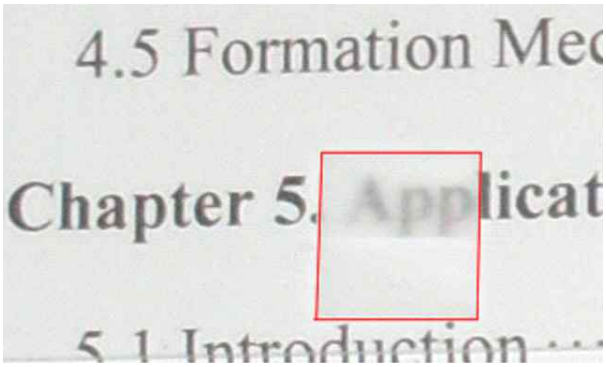

Figure 1.3 Photograph of the microstructured and unmodified soda-lime glass sample on the top of a printed document (red boundary indicates the microstructured sample area, whereas the remaining part is the unmodified sample area). (Ahsan *et al.*, 2013)

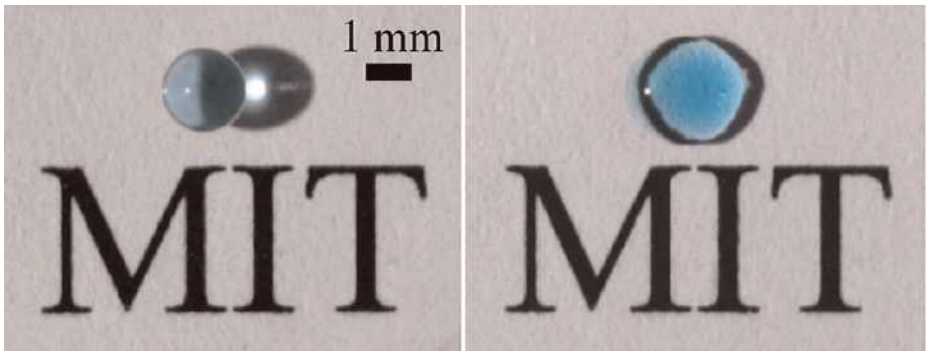

Figure 1.4 Blue-dyed water droplets sitting on a transparent nanotaper surface and on flat glass, each placed on top of printed black letters. (Park *et al.*, 2012)

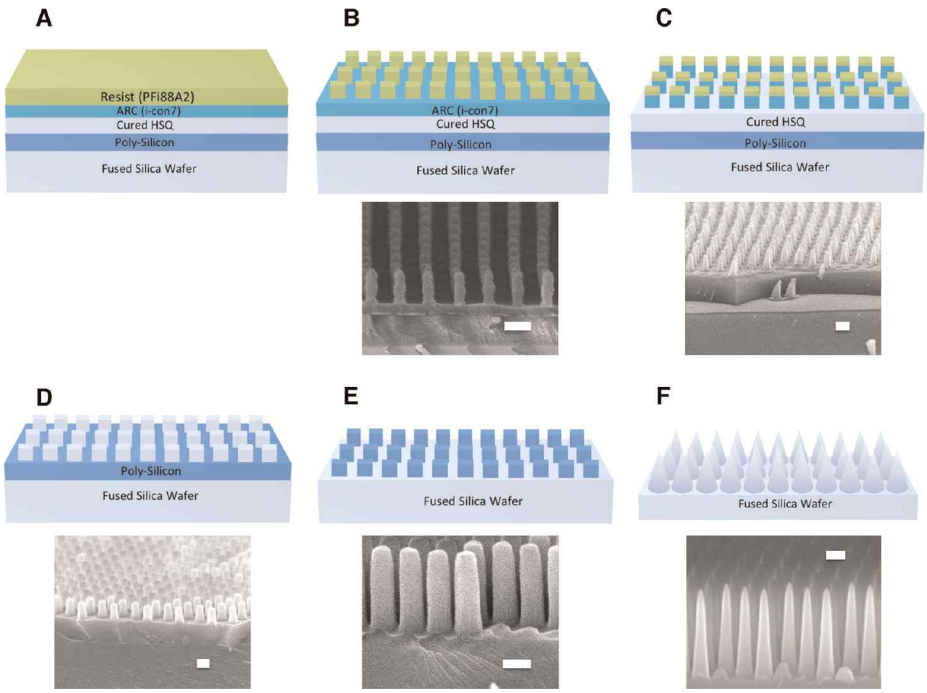

Figure 1.5 Stages of the fabrication process. (A) Deposition of multiple coating layers. (b) Development of photoresist pattern. (C-F) Subsequent etching steps of antireflective coating layer (C), cured HSQ layer (D), polysilicon layer (E), and fused silica wafer (F). All of the white scale bars on the micrographs represent 200 nm. (Park *et al.*, 2012)

2 Experimental details

2.1 Materials

Sulfuric acid (ACS reagent, 95.0-98.0%) and hydrogen peroxide (ACS reagent, 30 wt. % in H_2O) were obtained from Sigma Aldrich. 1*H*,1*H*,2*H*,2*H*-perfluorooctyl trichlorosilane (97%) and acetone (ACS reagent, ≥99.5%) were obtained from Sigma Aldrich. Ethylene glycol (ReagentPlus®, 99%) and hexadecane (anhydrous, ≥99%) were obtained from Sigma Aldrich. Silicon carbide (400 mesh particle size, ≥97.5%) were obtained from Sigma Aldrich. Soda-lime glass (76×26×1 mm) was obtained from Marienfeld. Petri Dish (35×10 mm) was obtained from SPL Life Sciences.

2.2 Preparation

To fabricate nanostructured glass, a 1 m thick SiO_2 overlayer was deposited onto the glass using plasma enhanced chemical vapor deposition (PECVD) with a mixture of N_2O gas and SiH_4 gas. Subsequently, the sample was etched using a glow discharge of CF_4 gas with various duration from 40 to 60 min by PECVD. The gas pressure and bias voltage were maintained at 30 mTorr and - 600 V, respectively. Finally, the sample was immersed in water to remove metal fluorides from the surface, and then dried with pure nitrogen gas. The sample is superhydrophilic due to nanostructure. [9]

1*H*,1*H*,2*H*,2*H*-perfluorooctyl trichlorosilane (PFOTS) was used

to reduce surface energy of the nanostructured glass by vapor deposition. Before silane coating, the nanostructured glass was immersed in piranha solution (3:1 mixture of concentrated sulfuric acid and 30 wt. % hydrogen peroxide solution) for 30 min. PFOTS was placed on the bottom of Petri dish and the nanostructured glass was placed on the inside of Petri dish lid by using double-sided tape. After deposition time 120 s, the nanostructured glass was thoroughly washed with acetone and dried with pure nitrogen gas. The result was glass exhibiting not only superhydrophobicity but also omniphobicity.

To fabricate hydrophobic glass, we proceeded with the same procedure that fabricates omniphobic glass, but bare glass was used instead of nanostructured glass.

To fabricate hydrophilic glass, bare glass was thoroughly washed with acetone, DI water and dried with pure nitrogen gas.

2.3 Measurement

Field-Emission Scanning Electron Microscope (SUPRA 55VP, Carl Zeiss) was used to observe surface nanostructures.

Perturbation solution of the Bashforth-Adams equation was used to calculate contact angles of water, ethylene glycol, and hexadecane [10].

Digital power & energy meter with Si photodiode power sensor (PM121D, Thorlabs) and 2 W, 532 nm diode-pumped solid-state laser with VD-IIIA DPSS laser driver were used to measure optical transmission.

VELOCICALC® air velocity meters (model 8346, TSI) was used to calculate velocity of external flow.

3 Surface fabrication

3.1 Fabrication of nanostructured glass

The SiO_2 layer was deposited onto glass as a sacrificial layer that was subsequently CF_4 plasma-treated to form a nanostructure by using a well-known anisotropic plasma etching technique, as shown in Figure 3.1.

Using SEM, It was found that the solid faction (dark area) and air fraction (bright area) increase and decrease with CF_4 plasma duration, respectively, as shown in Figure 3.2. The apparent contact angles for rough surface can be expressed as Cassie-Baxter equation [11]

$$\cos\theta_r = f_1 \cos\theta_f - f_2 \qquad (1)$$

where θ_r and θ_f are the contact angle of rough and flat surface, respectively, and f_1 and f_2 are the solid fraction and air fraction in solid and air compound surface, respectively. To achieve high contact angles of water, ethylene glycol and hexadecane on the nanostructured glass, it is necessary to decrease solid fraction and increase air fraction. Hence, it is natural to expect the contact angles of liquids on nanostructured glass to increase with decreasing CF_4 plasma duration. The results of our experiments show good agreement with the theoretical prediction, as will be shown later.

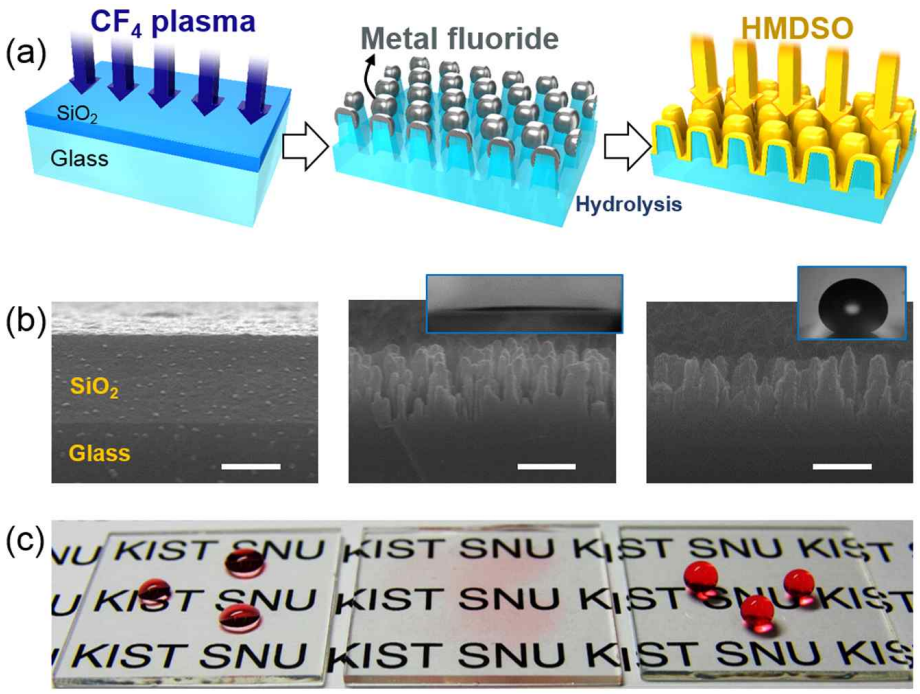

Figure 3.1 Schematic representation of the fabrication process of nanostructured glass. (a) Application of a sacrificial layer of SiO_2 and reactive ion etching by CF_4 plasma treatment. (b) Cross-sectional SEM images of SiO_2-coated glass before nanostructuring (left) and CF_4 plasma-etched glass with a SiO_2 coating before (middle) and after (right) pp-HMDSO coating. Scale bar is 500 nm. (c) Optical images of pristine (left), superhydrophilic (middle), and superhydrophobic (right) glass. Water was dyed red. (Yu *et al.*, 2015)

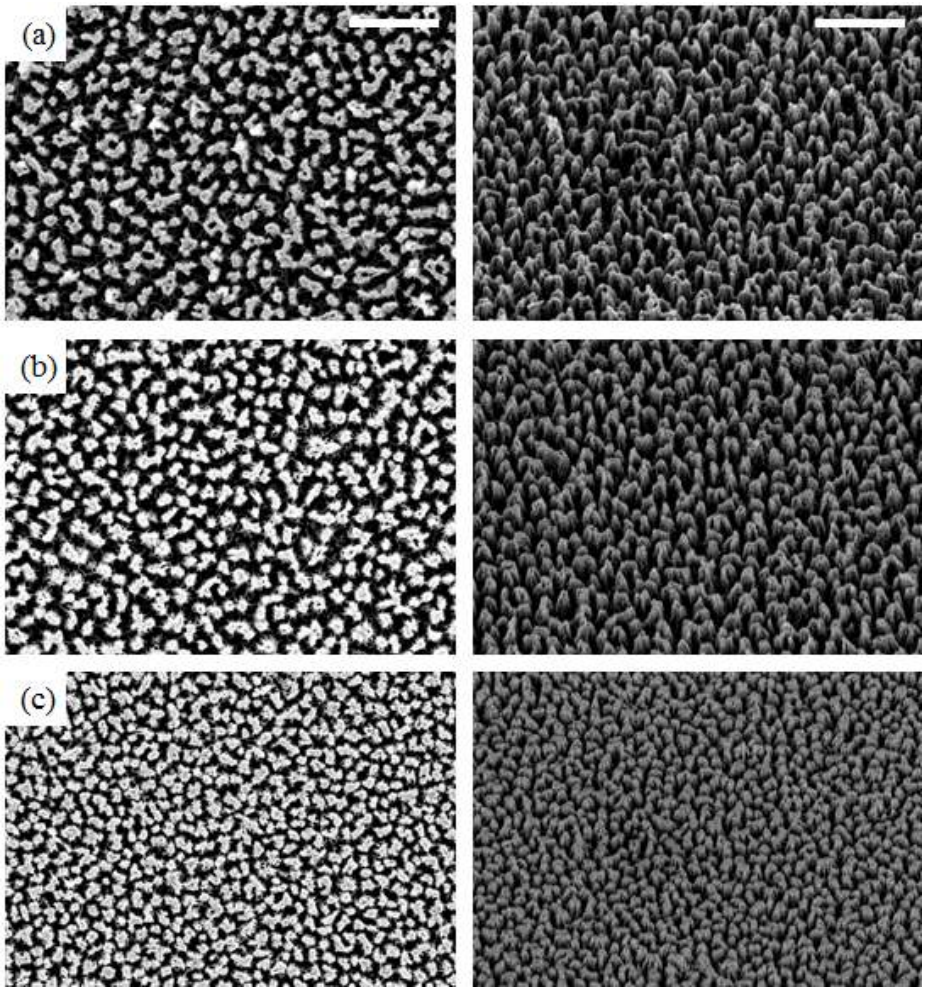

Figure 3.2 SEM top-view (left) and 40° tilted-view (right) images of nanostructure with various CF_4 plasma duration: (a) 40 min, (b) 50 min, and (c) 60 min. Scale bars are 1 μm.

3.2 Functionalization

Superhydrophobic, or omniphobic surfaces are obtained by silanization of micro- or nanostructured surface. We adopted 1*H*,1*H*,2*H*,2*H*-perfluorooctyl trichlorosilane (PFOTS) instead of hexamethyldisiloxane (HMDSO), since PFOTS has lower surface energy and better stability. [12]

It is well known that silane, a low-surface-energy material, reacts with hydroxyl group, as shown in Figure 3.3. There are two ways to functionalize surface with hydroxyl group: oxygen plasma and piranha solution. Since piranha solution is excellent for cleaning organic contaminants before silane coating, we choose piranha solution.

Since, however, it was reported that nanostructure may be deformed by piranha treatment before silane coating [13], as shown in Figure 3.4, it is necessary to observe nanostructure before and after piranha treatment. As shown in Figure 3.5, there is no difference in nanostructure with or without piranha treatment. Therefore, we confirmed that piranha treatment contributed solely to surface functionalization.

There is a possibility of enhanced silanization by temperature as well as hydroxyl group, since temperature has a significant influence on chemical reaction. To investigate the effect of temperature on silane coating, we set the experiment, as shown in Figure 3.6. The results of measurements of the contact angles of ethylene glycol and hexadecane on PFOTS-treated nanostructured glass with various temperature are shown in Figure 3.7. Water was omitted since PFOTS-treated nanostructured glass showed sufficient superhydrophobicity. The

contact angle of ethylene glycol increased from 143° to 155° at 65℃ and that of hexadecane was nearly constant. Therefore, we choose the coating temperature of 65℃.

Based on coating temperature, we evaluate the effects of the CF_4 plasma duration and PFOTS vapor deposition time on the contact angles of water, ethylene glycol and hexadecane, as shown in Figure 3.8. The contact angle of each liquid was found to increase with decreasing CF_4 plasma duration from 60 min to 40 min. As mentioned earlier, these results are in good agreement with theoretical prediction from Cassie-Baxter equation. In addition to CF_4 plasma duration, it was also found that the contact angle of each liquid increased with the PFOTS vapor deposition time and eventually saturated at 120 s.

Hence, we fabricated and optimized the omniphobic glass prepared by plasma etching. The nanostructured glass was etched with CF_4 plasma for 40 min. Subsequently, the nanostructured glass was immersed in piranha solution for 30 min, followed by PFOTS vapor deposition time of 120 s at 65℃. Contact angle of each liquid and photograph of optimized PFOTS-treated nanostructured glass are shown in Figure 3.9 and Figure 3.10, respectively.

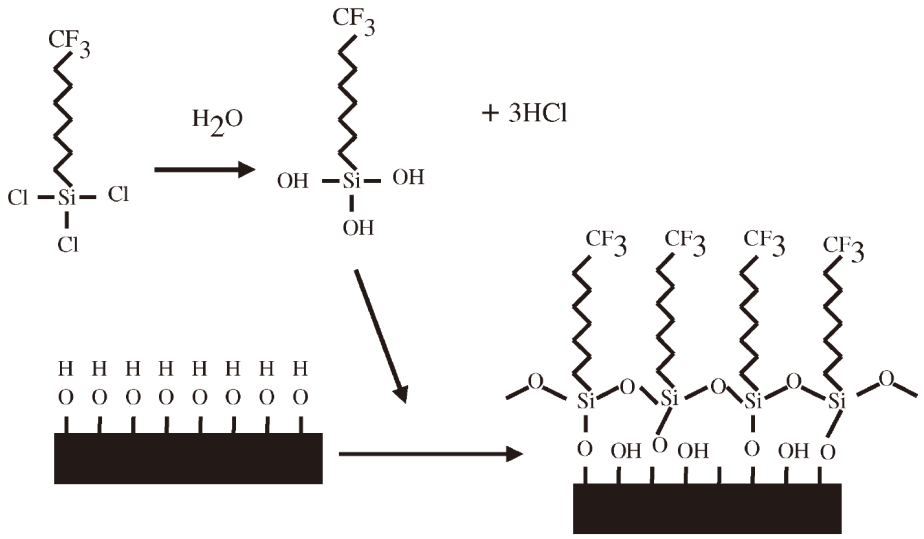

Figure 3.3 Formation mechanism of SAM on the hydroxylized silicon substrate. (Zhuang *et al.*, 2007)

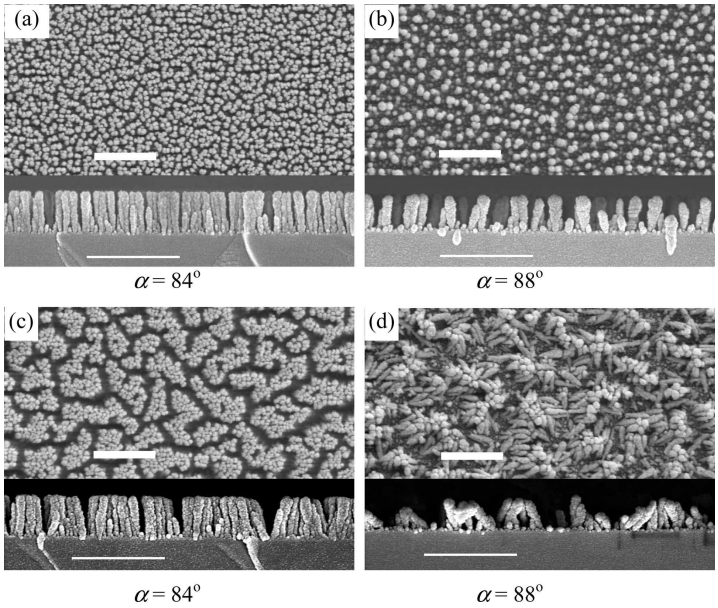

Figure 3.4 SEM top-view and cross-section images of Si nanorods grown at two different oblique angles: (a) before and (c) after piranha treatment for α = 84°; (b) before and (d) after piranha treatment for α = 88°. Scale bars = 1 μm. (Fan *et al.*, 2010)

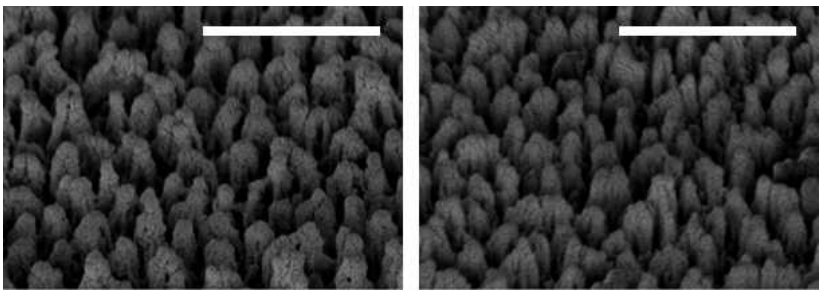

Figure 3.5 SEM 40° tilted-view images of nanostructure without piranha treatment (left) and with piranha treatment (right). Scale bars are 1 μm.

Figure 3.6 Experimental setup for temperature dependency for PFOTS vapor deposition.

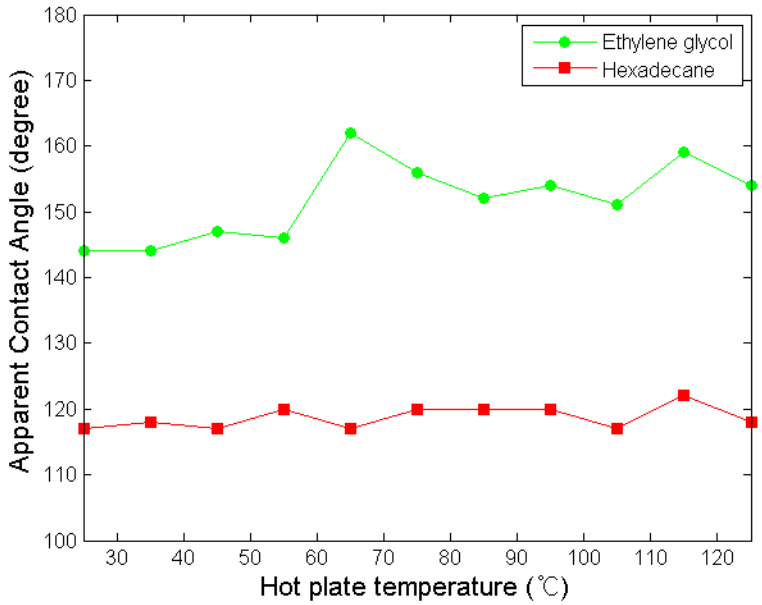

Figure 3.7 Contact angles of ethylene glycol and hexadecane on PFOTS-treated nanostructured glass with various temperature.

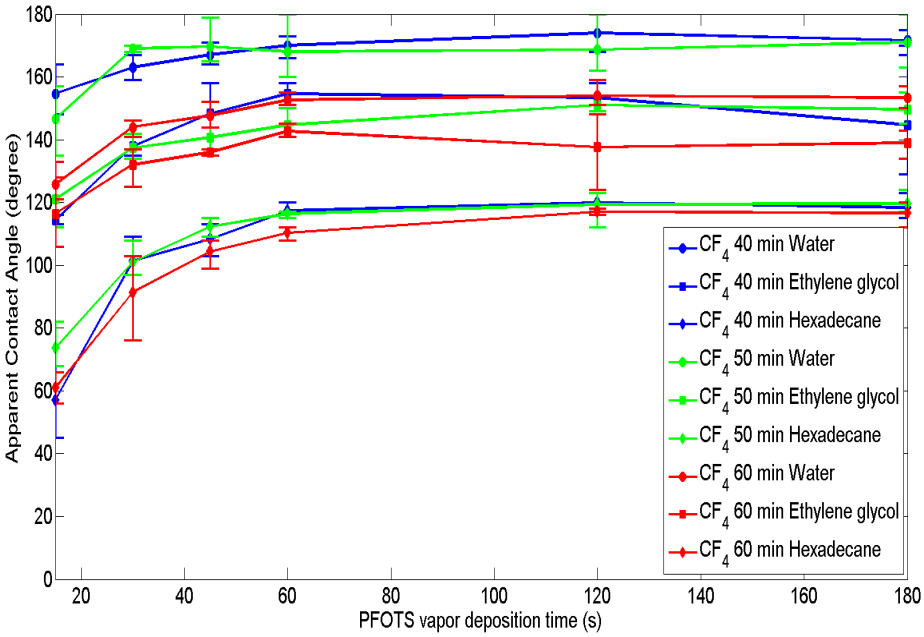

Figure 3.8 Contact angles of water, ethylene glycol, and hexadecane on PFOTS-treated nanostructured glass with various CF_4 plasma duration: 40 min (blue), 50 min (green), and 60 min (red).

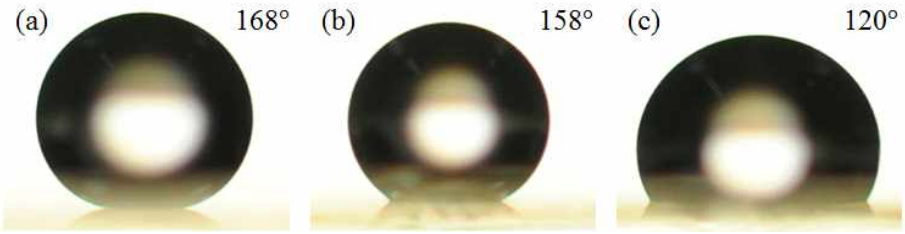

Figure 3.9 Contact angles of (a) water, (b) ethylene glycol, and (c) hexadecane on the optimized PFOTS-treated nanostructured glass.

Figure 3.10 Photograph of the optimized PFOTS-treated nanostructured glass. Scale bar is 10 mm.

4 Surface evaluation

4.1 Self-cleaning

To quantify the self-cleaning test, we choose silicon carbide (SiC) as contaminants, due to its hydrophilic property and similarity in shape and sizes to natural dirt [14]. We set up and quantify the self-cleaning test, as shown in Figure 4.1 and Figure 4.2, respectively.

It is interesting to note that hydrophobic glass was also cleaned by one droplet like superhydrophobic glass. However, there is notable difference in the surface before and after self-cleaning test, as shown in Figure 4.3.

On the superhydrophobic glass, Figure 4.3 (a), no residual water is formed as its water-repellent property, i.e. Lotus-effect. On the hydrophobic glass, residual water droplet is not formed on the place on which water droplets impact but formed on the below, as shown in Figure 4.3 (b). It is because hydrophobic glass shows moderate contact angle and contact angle hysteresis. On both hydrophilic, Figure 4.3 (c), and superhydrophilic, Figure 4.3 (d), residual water film is formed and considerable area is dirty with mixture of water and SiC.

Furthermore, when residual water evaporates, adhesion between contaminants and surface is reinforced so that it is difficult to remove particles from the surface. It was also reported that a visible but transparent layer of dissolved and subsequently re-crystallized salts had accumulated on glass samples that were never cleaned for seven month. These layers contributed

significantly to reduction in transmittance about 40% [15]. Therefore, considering that the residual water on the surface causes secondary effect, self-cleaning tests reveal that superhydrophobic (or omniphobic) glass show superior self-cleaning property and hydrophobic glass show partial self-cleaning property.

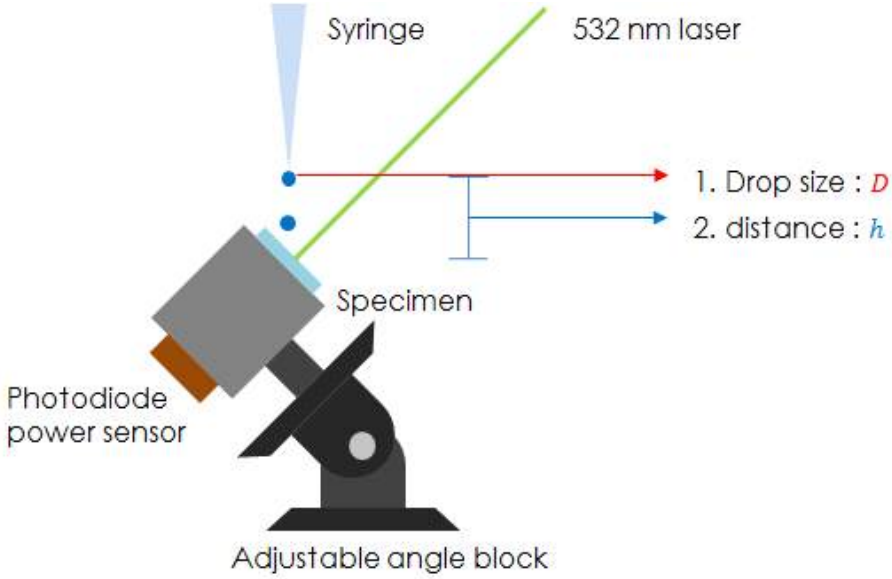

Figure 4.1 Experimental setup for self-cleaning.

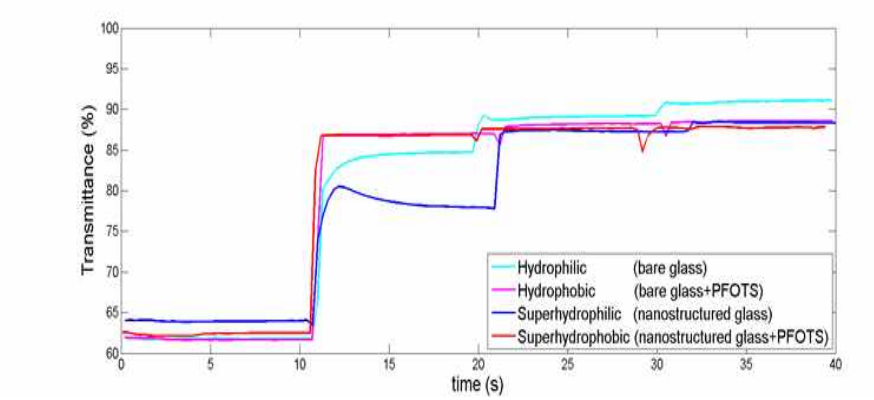

Figure 4.2 Evolution of optical transmission of 532 nm leaser through hydrophilic (cyan), hydrophobic (magenta), superhydrophilic (blue), and superhydrophobic (red) glass. Water droplets with a diameter of 4 mm were released onto glass tilted to 45° from a height 40 mm (corresponding $We = 42$) every 10 s.

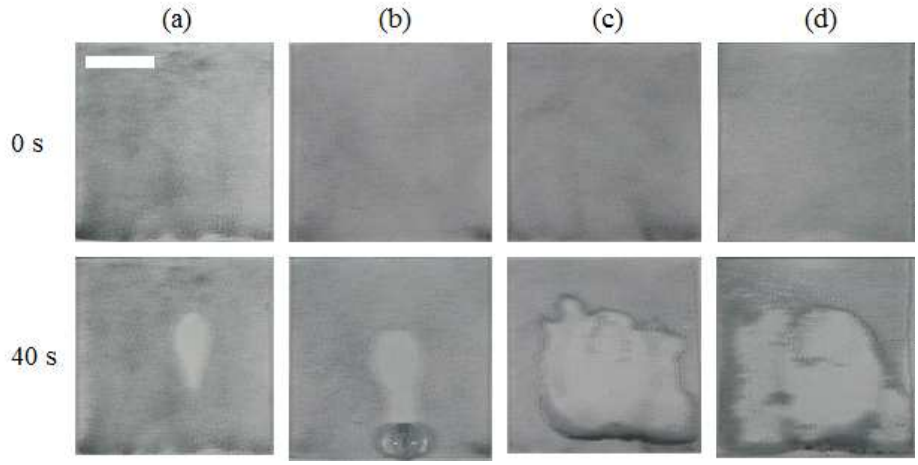

Figure 4.3 Self-cleaning test with time on (a) superhydrophobic, (b) hydrophobic, (c) hydrophilic, and (d) superhydrophilic glass. Scale bar is 10 mm.

4.2 Anti-fogging

To quantify the anti-fogging test, we choose ultrasonic humidifier. Air gun was used for external flow. We set up and quantify the anti-fogging test, as shown in Figure 4.4 and Figure 4.5, respectively.

Without external flow, optical transmission of superhydrophilic glass slightly decreased to 82% but those of superhydrophobic, hydrophobic, and hydrophilic glass decreased rapidly with time when we turned on ultrasonic humidifier. After turning off ultrasonic humidifier, optical transmission of superhydrophilic glass was immediately recovered, whereas those of superhydrophobic, hydrophobic, and hydrophilic glass increased slowly with time.

With external flow, notable difference could be observed. Optical transmissions of superhydrophilic and superhydrophobic glass slightly decreased to 90% and 78%, respectively, but those of hydrophobic and hydrophilic glass decreased rapidly with time when we turned on ultrasonic humidifier. After turning off ultrasonic humidifier, optical transmission of superhydrophilic and superhydrophobic glass were immediately recovered, whereas those of hydrophobic and hydrophilic glass increased slowly with time.

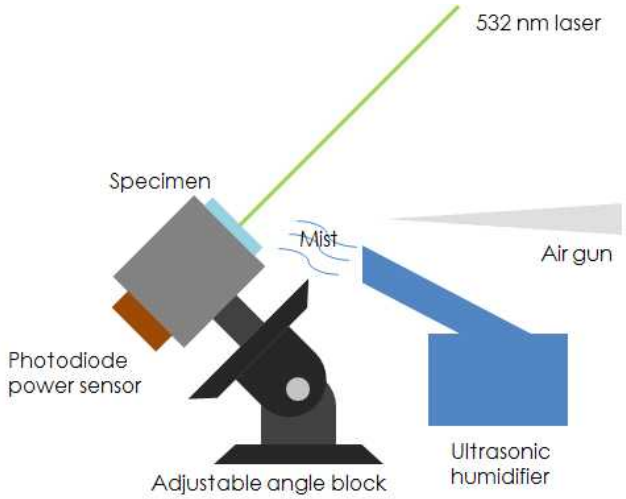

Figure 4.4 Experimental setup for anti-fogging.

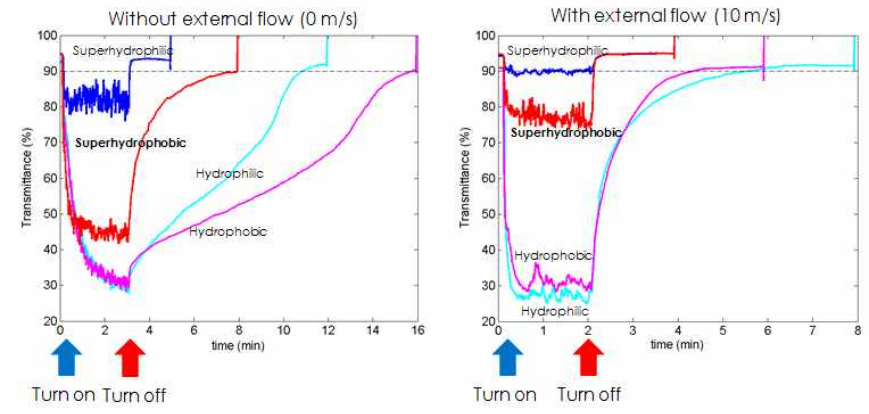

Figure 4.5 Evolution of optical transmission of 532 nm leaser through hydrophilic (cyan), hydrophobic (magenta), superhydrophilic (blue), and superhydrophobic (red) glass without external flow (left) and with external flow (right).

	Hydrophilic		Hydrophobic		Super hydrophilic		Super hydrophobic	
Flow (m/s)	0	10	0	10	0	10	0	10
Ref. TR (%)	92.3	90.7	92.7	91	94.5	94	95	94.5
Fogging TR (%)	31	28	32	33	82	90	46	78
Recover time (s)	460	150	760	125	2	1	290	3

Table 1 The results of quantification of anti-fogging. Ref. TR and Fogging TR refer to optical transmission of glass before anti-fogging test and that of glass during anti-fogging test, respectively. Recover time is the time it takes for the glass to recover optical transmission to 90%.

5 Conclusions

We fabricated, optimized and evaluated omniphobic transparent glass by using non-lithographic, anisotropic etching. To fabricated nanostructured glass, optimized CF_4 plasma duration is 40 min. To functionalize the nanostructured glass with PFOTS, optimized temperature and vapor deposition time are 65℃ and 120 s, respectively.

Based on the optimized omniphobic transparent glass, we evaluated self-cleaning and anti-fogging. Since the residual water on the surface may cause secondary effect such as coagulation, superhydrophobic (or omniphobic) glass show superior self-cleaning property. Also superhydrophobic glass subjected to external flow show anti-fogging property, even though superhydrophilic glass show anti-fogging property regardless of external flow.

Considering both self-cleaning and anti-fogging property, superhydrophobic (or omniphobic) glass is superior to superhydrophilic glass. The process we developed in this work can be used to fabricate such products as eyeglasses, solar pannel and optical instruments, where minimization of contamination is crucial.

References

1 W. Barthlott and C. Neinhuis. Purity of the sacred lotus, or escape from contamination in biological surfaces. *Planta* 1997, 202, 1-8

2 X. Gao and L. Jiang. Biophysics: water-repellent legs of water striders. *Nature* 2004, 432, 36

3 X. Gao, X. Yan, X. Yao, L. Xu, K. K. Zhang, J. Zhang, B. Yang, and L. Jiang. The dry-style antifogging properties of mosquito compound eyes and artificial analogues prepared by soft lithography. *Advanced Materials* 2007, 19, 2213-2217

4 M. S. Ahsan, F. Dewanada, M.S. Lee, H. Sekita, and T. Sumiyoshi. Formation of superhydrophobic soda-lime glass surface using femtosecond laser pulses. *Applied Surface Science* 2013, 265 784-789

5 X. Y. Ling, I. Y. Phang, G. J. Vancso, J. Huskens, and D. N. Reinhoudt. Stable and transparent superhydrophobic nanoparticle films. *Langmuir* 2009, 25, 3260-3263

6 L. Cao and D. Gao. Transparent superhydrophobic and highly oleophobic coatings. *Faraday Discussions* 2010, 146, 57-65

7 D. Kontziampasis, G. Boulousis, A. Smyrnakis, K. Ellinas, A. Tserepi, and E. Gogolides. Biomimetic, antireflective, superhydrophobic and oloephobic PMMA and PMMA-coated glass

surfaces fabricated by plasma processing. *Microelectronic Engineering* 2014, 121, 33-38

8 K.-C. Park, H.J. Choi, C.H. Chang, R. E. Cohen, G. H. McKinley, and G. Barbastathis. Nanotextured silica surfaces with robust superhydrophobicity and omnidirectional broadband supertransmissivity. *Acs Nano* 2012, 6, 3789-3799

9 E. Yu, S.C. Kim, H.J. Lee, K.H. Oh, and M.-W. Moon. Extreme wettability of nanostructured glass fabricated by non-lithographic anisotropic etching. *Scientific Reports* 2015, 5, 9362

10 S. Srinivasan, G. H. McKinley, and R. E. Cohen. Assessing the accuracy of contact angle measurements for sessile drops on liquid-repellent surfaces. *Langmuir* 2011 27, 13582-13589

11 A. B. D. Cassie and S. Baxter. Wettability of porous surfaces. *Transactions of the Faraday Society* 1944, 40, 546

12 Y. X. Zhuang, O. Hansen, T. Knieling, C. Wang, P. Rombach, W. Lang, W. Benecke, M. Kehlenbeck, and J. Koblitz. Thermal stability of vapor phase deposited self-assembled monolayers for MEMS anti-stiction. *Journal of Micromechanics and Microengineering* 2006, 16, 2259-2264

13 J. Fan and Y. Zhao. Nanocarpet effect induced superhydrophobicity. *Langmuir* 2010, 26, 8245-8250

14 B. Bhushan, Y.C. Jung, and K. Koch. Self-cleaning efficiency of artificial superhydrophobic surfaces. *Langmuir* 2009, 25, 3240-3248

15 H. K. Elminir, A. E. Ghitas, R. H. Hamid, F. El-Hussainy, M. M. Beheary, and K. M. Abdel-Moneim. Effect of dust on the transparent cover of solar collectors. *Energy conversion and management* 2006, 47, 3192-3203

요약(국문초록)

물의 접촉각이 150도 이상이고 매우 낮은 이력각을 갖는 초소수성 표면은 연꽃 효과라고도 불리는 자가세정 기능을 갖는다. 하지만 초소수성 표면은 기름 오염에 취약하고 오염될 경우 자가세정 성능이 떨어지게 된다. 따라서 표면이 초소수성일 뿐만 아니라 소유성일 필요가 있다. 본 연구에서는 리소그래피를 사용하지 않고 비등방성 식각을 이용하여 투명한 omniphobic 유리를 제작, 최적화 및 평가를 하였다. 표면 거칠기와 낮은 표면 에너지를 가하기 위해 CF_4 가스의 글로 방전과 1*H*,1*H*,2*H*,2*H*-perfluorooctyl trichlorosilane (PFOTS)가 각각 사용되었다. 본 연구에서 우리는 온도, CF_4 플라즈마 식각 시간 및 PFOTS 증기 증착 시간이 물, 에틸렌글리콜 그리고 헥사데케인의 접촉각에 미치는 영향을 조사하였고 측정된 접촉각의 결과와 Cassie and Baxter의 이론과 비교하였다. 그리고 자가세정과 김서림 방지를 정량화하기 위해 초소수성, 소수성, 초친수성, 친수성 유리의 광투과도를 측정하였다.

주요어 : 초소수성, omniphobic, 유리, 플라즈마, 자가세정, 김서림 방지
학 번 : 2013-23071